



ELSEVIER

Journal of Alloys and Compounds 275–277 (1998) 852–858

Journal of  
ALLOYS  
AND COMPOUNDS

## Two high and low symmetry europium complexes with L-proline: Spectroscopy and structure

Ewa Huskowska<sup>a</sup>, Ilona Turowska-Tyrk<sup>b</sup>, Janina Legendziewicz<sup>a,\*</sup>, Tadeusz Głowiak<sup>a</sup><sup>a</sup>Faculty of Chemistry, University of Wrocław, 14 F. Joliot-Curie Str., 50-383 Wrocław, Poland<sup>b</sup>Institute of Physical and Theoretical Chemistry, Wrocław University of Technology, Wybrzeże Wyspiańskiego 27, 50-370 Wrocław, Poland

### Abstract

Lanthanide ions are widely applied as spectroscopic probes in studies of biomolecular structures. However, in all known crystal structures of lanthanide complexes with amino acids and peptides, dimers and polymers are formed with one or more symmetry sites of the metal ions; this strongly affects the spectroscopic properties. In order to explain the role of the type of amino acid, the Ln/ligand ratio and ligand chirality in the structure, two types of Eu(III) complexes with L-proline of formulae  $[\text{Eu}_2(\text{C}_5\text{H}_9\text{O}_2\text{N})_4(\text{H}_2\text{O})_8](\text{ClO}_4)_6 \cdot 4\text{H}_2\text{O}$  (**I**) and  $[\text{Eu}(\text{C}_5\text{H}_9\text{O}_2\text{N})_3(\text{H}_2\text{O})_3](\text{ClO}_4)_3$  (**II**) were obtained and characterised by X-ray and electron spectroscopic methods. Compound **I** crystallizes in a tetragonal space group ( $P4_2,2$ ) and forms dimers with two nonequivalent europium sites, with square antiprism polyhedra. Compound **II** (triclinic  $P1$ ) forms polymeric chains in a crystal lattice, with two coordination modes of the proline molecules (mono- and bridging bidentate) and with dodecahedron polyhedra. Moreover, differences in the Eu–O bond lengths between two crystallographically nonequivalent metal ions are smaller in structure **II**. High resolution absorption, excitation and emission spectra of the compounds were measured at 4–293 K and analysed in order to explain how subtle structural changes affect the intensity of the electronic transitions, splitting of levels and vibronic coupling. © 1998 Published by Elsevier Science S.A.

**Keywords:** Absorption spectroscopy; Crystal structure; Europium; Luminescence; Proline

### 1. Introduction

In the last 10 years, we have investigated the crystal structures of a series of lanthanide compounds with amino acids, their phosphonic analogues and peptides [1–8]. It was found that their subtle architecture depends on: the metal-to-ligand ratio, the ligand chirality, the lanthanide ionic radius and the type of amino acid (mono or dicarboxylate). This was mainly manifested in differences of the dimer or polymer type, the kind of coordination mode as well as in changes in the symmetry of the dimeric units. Investigations of the above systems throw light on the wide preparation possibilities of different forms of complexes, which can aid in understanding their structure in solution.

The aim of the present study is to focus on the effect of system composition on the structure and symmetry and to explain how the dimer or polymer structure modifies the spectroscopic characteristics of the system.

### 2. Experimental

Crystals of the compounds were grown from an aqueous solution with a Me/L=1:1 molar ratio at  $\text{pH} \approx 4$ , similar to the procedure described in Ref. [4]. Two types of crystals of different shape and composition were obtained:  $[\text{Eu}_2(\text{L-pro})_4(\text{H}_2\text{O})_8](\text{ClO}_4)_6 \cdot 4\text{H}_2\text{O}$  (**I**) and  $[\text{Eu}(\text{L-pro})_3(\text{H}_2\text{O})_3](\text{ClO}_4)_3$  (**II**). Absorption spectra at 293, 50 and 4 K were recorded on a Cary-Varian 5 spectrophotometer equipped with a helium flow cryostat (Oxford CF 1204) in the region 280–600 nm. The intensities of the f–f transitions were calculated by integration of the Gauss–Lorentzian curve and transformed to oscillator strength values using the ICH 10 program. Excitation and emission spectra were recorded at 293, 77 and 4 K using a SLM Aminco SPF 500 spectrofluorometer.

#### 2.1. X-ray measurements

Crystals of **I** and **II** were examined with graphite-monochromated Mo  $K\alpha$  radiation on a Kuma KM-4 diffractometer at 293 K. Precise values of the unit cell parameters were determined by least-squares treatment of

\*Corresponding author. Fax: +48 71 3282348; e-mail: jl@wchuwr.chem.uni.wroc.pl

the setting angles of 25 reflections. For both crystals, profiles of reflections were measured using a  $\theta$ – $2\theta$  scan technique. The data were corrected for Lorentz-polarization and absorption ( $\psi$  scans) effects. Structure **I** was solved by direct methods and **II** by Patterson techniques from the SHELXS86 program [9]. The positions of most of the non-hydrogen atoms were revealed. The remaining atoms were found from several difference Fourier maps.

In **I** the Eu atoms are situated on a four-fold axis and one of the perchlorate anions on a two-fold axis. For the proline ring in **I** and four rings in **II**, very large temperature factors and deviations from the expected geometry are observed, which suggests a disorder problem. Careful studies revealed two orientations (conformations) of the rings, both of which were refined with some restraints. Most of the restraints were released in the final stages of the refinement. The occupancies of the rings were refined to final values of 53 and 47% for **I** and 68, 58, 67 and 77% for the dominating conformations of the four rings of **II**. All non-hydrogen atoms of **I** were refined anisotropically by the use of SHELXL93 [10]. For **II** the disordered atoms were treated isotropically. The positions of the H atoms in the pyrrolidine ring of **I** were calculated and refined using constraints for two conformations. In the case of **II** only H atoms for the fragment of the larger occupancy were taken into account. The hydrogen atoms in water molecules were not seen clearly by the difference synthesis and were not used in the refinement. Final cell constants, details of data

collection and the refinement process for **I** and **II** are given in Table 1. Final atomic coordinates have been deposited at the Cambridge Crystallographic Data Centre.

### 3. Results and discussion

The molecular structures of **I** and **II** with the numbering scheme for atoms are displayed in Figs. 1 and 2, respectively. Selected interatomic distances for both compounds are given in Table 2. Compound **I** is a dimer situated on a four-fold axis, whereas compound **II** forms linear polymers along the [100] direction in the crystal lattice. Polymeric chains with a somewhat different composition were also observed in neodymium [4], holmium and dysprosium crystals of complexes with L-proline [5].

The Eu–Eu distance within the **I** dimer is 4.348(3) Å and that between the dimers 5.879(4) Å. The two europium ions are bridged by four crystallographically equivalent carboxyl groups from the proline molecules and additionally coordinated by four equivalent water molecules creating in this way two polyhedra which can be described as square antiprisms. The two faces of both polyhedra are formed by four water and by four carboxylate oxygen atoms.

Each pair of adjacent metal ions in structure **II** is bridged by two carboxyl groups from the proline molecules. Additionally, each europium ion is connected to one

Table 1  
Crystal data and structure refinement

Compound:	$C_{20}H_{60}Cl_6Eu_2N_4O_{44}$	$C_{15}H_{33}Cl_3EuN_3O_{21}$
$M_r$	1577.34	849.75
$T$	293(2) K	293(2) K
$\lambda$	0.71073 Å	0.71073 Å
Crystal system	Tetragonal	Triclinic
Space group	$P4_2,2$	$P1$
Unit cell dimensions	$a=b=16.176(12)$ Å, $c=10.227(7)$ Å	$a=9.924(3)$ Å, $b=13.033(5)$ Å, $c=13.791(7)$ Å $\alpha=62.36(4)^\circ$ , $\beta=68.08(4)^\circ$ , $\gamma=79.20(3)^\circ$
$V$	$2676(3)$ Å <sup>3</sup>	$1465.7(10)$ Å <sup>3</sup>
$Z$	2	2
$D_x$	$1.958$ Mg m <sup>-3</sup>	$1.925$ Mg m <sup>-3</sup>
$\mu$	$2.739$ mm <sup>-1</sup>	$2.506$ mm <sup>-1</sup>
$F(000)$	1576	852
Crystal size	$0.40 \times 0.55 \times 0.55$ mm	$0.35 \times 0.55 \times 0.55$ mm
$\theta_{max}$	$26.0^\circ$	$26.0^\circ$
Index ranges	$-20 \leq h \leq 24$ , $0 \leq k \leq 24$ , $-15 \leq l \leq 0$	$-11 \leq h \leq 12$ , $-14 \leq k \leq 15$ , $0 \leq l \leq 15$
Reflections collected	3385	5972
Independent reflections	2642	5972
$R_{int}$	0.085	0
$S$	1.12	1.13
$R$ indices [ $I > 2\sigma(I)$ ]	$R_1=0.048$ , $wR_2=0.131$	$R_1=0.040$ , $wR_2=0.102$
$R$ indices (all data)	$R_1=0.069$ , $wR_2=0.152$	$R_1=0.044$ , $wR_2=0.108$
Absolute structure	0.01(5)	0.01(2)
Extinction coefficient	0.0029(5)	0.0111(10)
$\Delta\rho_{max}$ , $\Delta\rho_{min}$	$0.72$ e Å <sup>-3</sup> , $-1.16$ e Å <sup>-3</sup> (close to Eu)	$2.11$ e Å <sup>-3</sup> , $-2.21$ e Å <sup>-3</sup> (close to Eu)

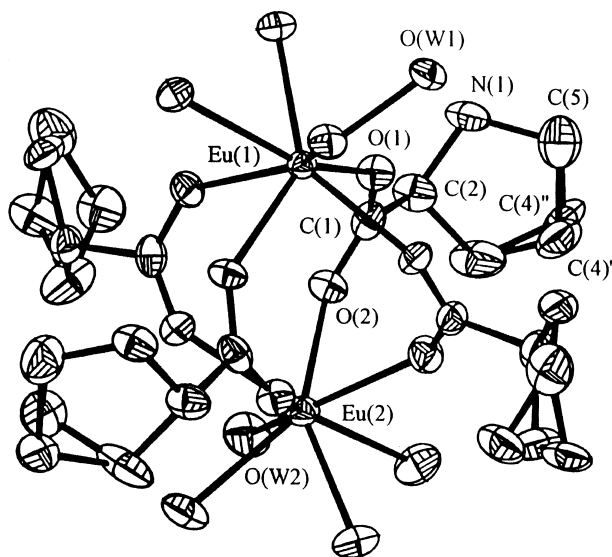


Fig. 1. ORTEP [11] diagram for **I**. Ellipsoids are drawn at the 50% probability level. Atomic labels for the asymmetric unit are displayed.

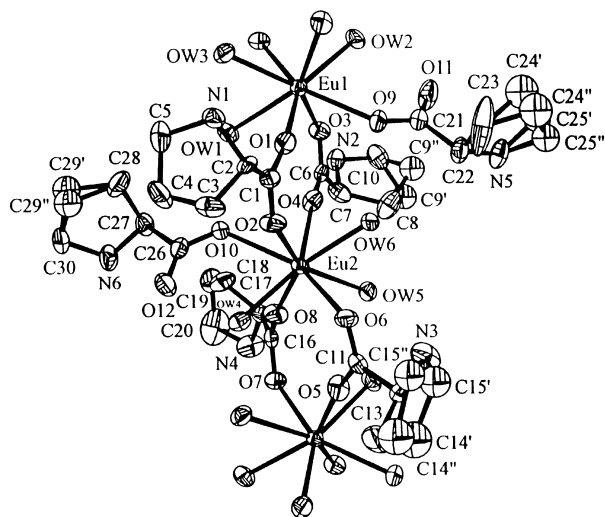


Fig. 2. ORTEP [11] diagram for **II**. Ellipsoids are drawn at the 50% probability level. Atomic labels for the asymmetric unit are displayed.

oxygen atom of the proline carboxyl group and to three water molecules. The europium ions in the chains repeat every 4.966(2) and 5.031(2) Å. The strength of the M–M intradimer or chain coupling is given by the number of carboxylate bridges formed; this is well manifested in these systems since both contain the same ligands.

In the case of structure **II**, the eight coordinating oxygen atoms form slightly distorted dodecahedra. The symmetry deviation parameter  $\Delta$ , defined as the mean square distance between the observed and ideal positions of the atoms in the antiprism, is 0.038 and 0.024 Å<sup>2</sup> for the two europium ions in **I** and 0.048 and 0.028 Å<sup>2</sup> for dodecahedra in **II**. However, the differences in the Eu–O bond lengths between two crystallographically nonequivalent metal ions are smaller in structure **II**: the mean Eu–O distances are 2.369(6) and 2.406(5) Å for the two polyhedra of **I** and 2.406(3) and 2.426(3) Å for **II**.

It should be mentioned that the number of proline molecules in the complexes leads to different modifications of the structures and modulates the type of carboxyl group coordination. Furthermore, for the same conditions of synthesis as for the present compounds, crystals of different composition have been obtained [4]. Light lanthanides had the formula  $[\text{Ln}(\text{L-pro})_3(\text{H}_2\text{O})_2](\text{ClO}_4)_3$  and contained a polymer consisting of dimeric subunits, whereas heavy lanthanides had the formula  $[\text{Ln}(\text{L-pro})_2(\text{H}_2\text{O})_5](\text{ClO}_4)_3$  and formed a linear polymer. Eu, as a member of the middle of the lanthanide series (ionic radius 1.07 Å for CN=8) [12], forms, under the same conditions, two complexes simultaneously with M/L-pro ratios of 1:3 and 1:2. These complexes preserve the same CN=8, but differ in the number of coordinated water molecules and the coordination of proline in comparison with relevant complexes of light and heavy lanthanides. This shows that subtle changes in the ionic radii of lanthanide ions can influence the structure of the complexes. As a consequence we obtained two types of complexes: **I**, with unexpected high tetragonal crystallographic symmetry (previously unknown for lanthanide–amino acids

Table 2

Selected interatomic distances (Å) for compounds **I** and **II**

Atoms	Bond	Atoms	Bond	Atoms	Bond
<b>Compound I</b>					
Eu(1)–O(W1)	2.454(7)	Eu2–O(W2)	2.417(8)	O(1)–C(1)	1.268(13)
Eu(1)–O(1)	2.358(7)	Eu(2)–O(2)	2.321(8)	O(2)–C(1)	1.228(13)
<b>Compound II</b>					
Eu(1)–O(5)	2.323(9)	Eu(1)–OW2	2.509(9)	Eu(2)–O(6) <sup>b</sup>	2.425(10)
Eu(1)–O(1)	2.331(9)	Eu(1)–OW3	2.527(10)	Eu(2)–OW6	2.444(9)
Eu(1)–O(3)	2.391(9)	Eu(2)–O(8)	2.318(9)	Eu(2)–OW4	2.461(9)
Eu(1)–O(7) <sup>a</sup>	2.414(10)	Eu(2)–O(4)	2.323(9)	Eu(2)–O(10)	2.516(10)
Eu(1)–O(9)	2.444(10)	Eu(2)–O(2)	2.348(9)	O(1)–C(1)	1.26(2)
Eu(1)–OW1	2.467(10)	Eu(2)–OW5	2.416(10)	O(2)–C(1)	1.24(2)

Symmetry transformations used to generate equivalent atoms:

<sup>a</sup> =  $x - 1, y, z$ .

<sup>b</sup> =  $x + 1, y, z$ .

systems); and **II**, with a triclinic structure as for many other lanthanide systems.

It is also worth pointing out that the separation of the europium ions in the dimer of structure **I** is slightly smaller in comparison with the similar dimer in the complex with L-alanine,  $[\text{Ln}_2(\text{L-ala})_4(\text{H}_2\text{O})_8](\text{ClO}_4)_6$  [13]. Furthermore, in  $[\text{Nd}(\text{L-pro})_3(\text{H}_2\text{O})_2](\text{ClO}_4)_3$ , where the one-dimensional polymer is composed of dimeric subunits with four carboxyl bridges, the separation (4.590 Å before and 4.490 Å after correction for the  $\text{Eu}^{3+}$  ionic radii) is also not comparable [4].

### 3.1. Spectroscopic results

X-ray analysis has shown the formation of dimers and polymers with different M–M distances and different symmetry of the europium ions for both systems. In addition, more pronounced changes in the M–O bond lengths for the two europium ions in noncentrosymmetric dimeric units in structure **I** were observed ( $\Delta d_{\text{Eu(I)}}=0.037$ ,  $\Delta d_{\text{Eu(II)}}=0.020$  Å).

Which of the above factors strongly affects the spectroscopy of the systems? Figs. 3 and 4 show absorption spectra of **I** and **II** at room temperature. Table 3 shows oscillator strength values calculated in the range of f–f transitions. For compound **I** they were evaluated from spectra along *a* and from  $\sigma$  and  $\pi$  polarized spectra along the *c*-axis; for compound **II** they were evaluated from the spectra of a single crystal oriented in three directions. Note that for compound **I** polarization of light leads to only two components remaining in the  ${}^7\text{F}_0 \rightarrow {}^5\text{D}_2$  transition for orientation *c*.

In the region of the  ${}^7\text{F}_0 \rightarrow {}^5\text{D}_0$  transitions two components were detected for compound **I** with  $6\text{ cm}^{-1}$  half band width, which confirms the existence of two nonequivalent metal ion positions in the noncentrosymmetric dimer. Furthermore, these bands are shifted from each other by  $18\text{ cm}^{-1}$ , showing a stronger splitting of the levels for one  $\text{Eu}^{3+}$  centre. Thus, the separated components for these two structural positions were easily recorded even at room temperature. In contrast, the  ${}^7\text{F}_0 \rightarrow {}^5\text{D}_0$  transition of compound **II** is a single asymmetric

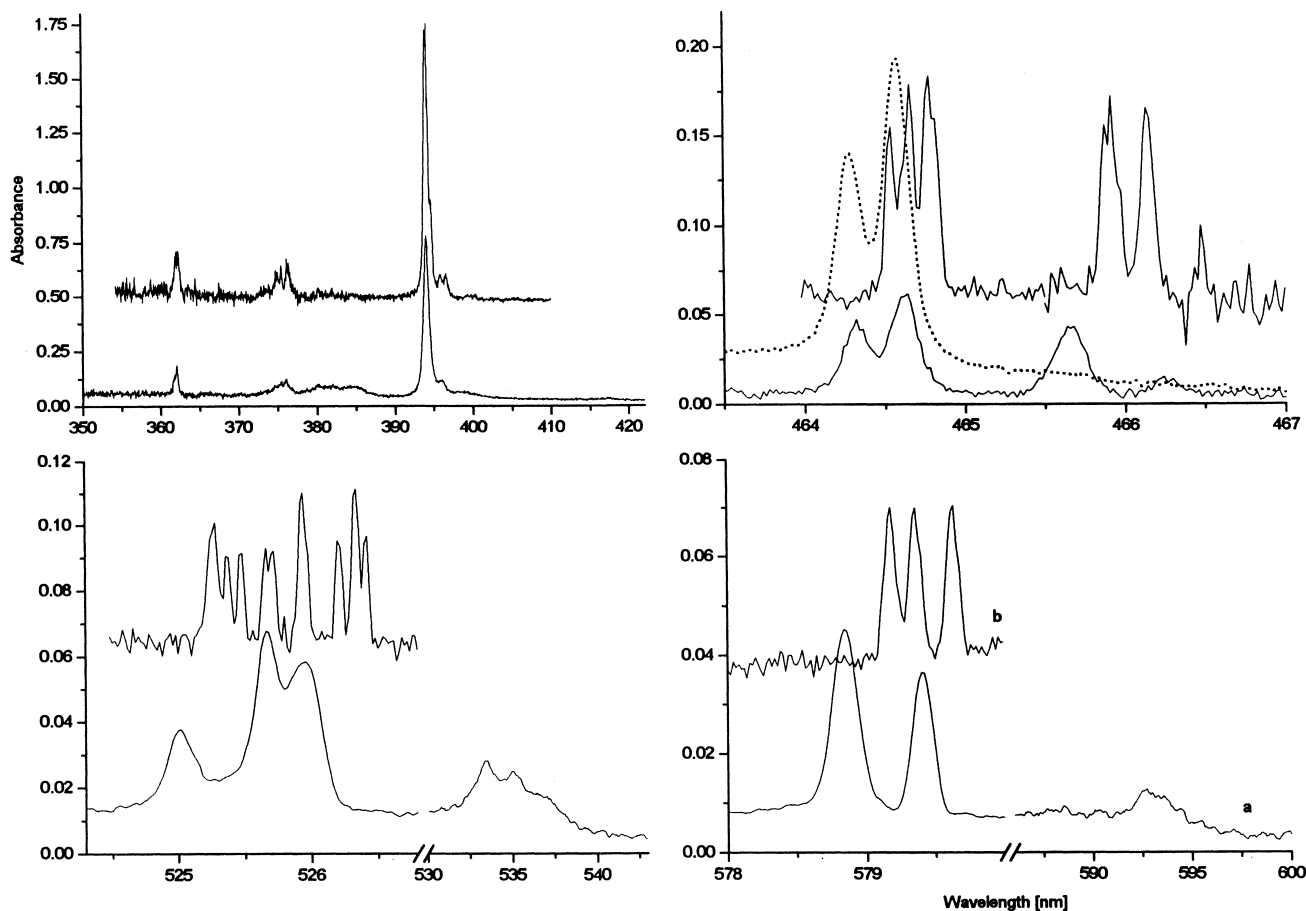


Fig. 3. Absorption spectra of a  $[\text{Eu}_2(\text{C}_5\text{H}_9\text{O}_2\text{N})_4(\text{H}_2\text{O})_8](\text{ClO}_4)_6 \cdot 4\text{H}_2\text{O}$  single crystal at (a) 293 K (along the *a*-axis, dotted line along the *c*-axis) and (b) 4 K.

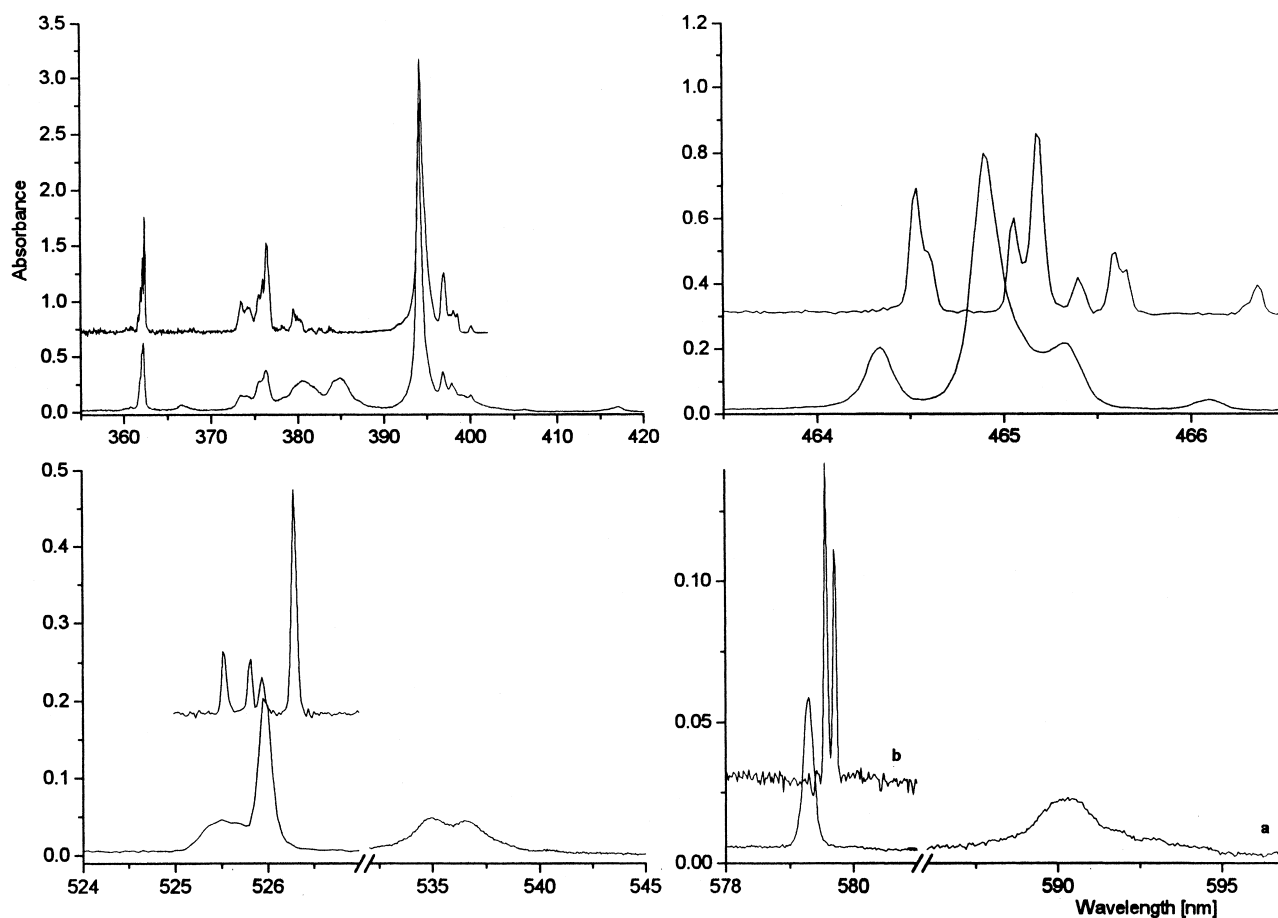


Fig. 4. Absorption spectra of a  $[\text{Eu}(\text{C}_5\text{H}_9\text{O}_2\text{N})_3(\text{H}_2\text{O})_3](\text{ClO}_4)_3$  single crystal at (a) 293 K and (b) 4 K.

band with an almost undetectable shoulder. From X-ray analysis it has been found that the difference in the  $\Delta$  parameter for the two  $\text{Eu}^{3+}$  ions is larger than for

compound **I**, but the differences in the M–L bond lengths are smaller.

Intensity analysis of the f–f transitions confirms the

Table 3

Oscillator strength values ( $P \times 10^8$ ) of the f–f transition in single crystal spectra of compounds **I** and **II** at 293 and 4 K

Transition	Spectral region (nm)	$[\text{Eu}_2(\text{C}_5\text{H}_9\text{O}_2\text{N})_4(\text{H}_2\text{O})_8](\text{ClO}_4)_6 \cdot 4\text{H}_2\text{O}$			$[\text{Eu}(\text{C}_5\text{H}_9\text{O}_2\text{N})_3(\text{H}_2\text{O})_3](\text{ClO}_4)_3$		
		$P$ dir <i>a</i>	$P$ dir <i>a</i> , 4 K	$P_{\text{mean}}$ , RT	$P$ dir <i>c</i>	$P$ dir <i>c</i> , 4 K	$P_{\text{mean}}$ , RT
${}^7\text{F}_1 \rightarrow {}^5\text{D}_0$	580–596	0.8		0.7	1.1		1.1
${}^7\text{F}_0 \rightarrow {}^5\text{D}_0$	579–585	0.68 <sup>a</sup>	0.65	0.45	0.30 <sup>a</sup>	0.26	0.22
${}^7\text{F}_1 \rightarrow {}^5\text{D}_1$	530–542	3.6		3.5	4.1		4.0
${}^7\text{F}_0 \rightarrow {}^5\text{D}_1$	524–527	1.7 <sup>a</sup>	1.7	1.6	1.8 <sup>a</sup>	0.86	1.32
${}^7\text{F}_0 \rightarrow {}^5\text{D}_2$	463–467	3.9	3.8	4.9	8.9	4.7	8.4
${}^7\text{F}_1 \rightarrow {}^5\text{D}_3$	412–418	1.6		1.7	3.9		3.3
${}^7\text{F}_0 \rightarrow {}^5\text{L}_6$	390–410	144.6	148.3	163.8	167.3	144.4	164.2
${}^7\text{F}_1 \rightarrow {}^5\text{G}_2$	385–395	31.4		35.8	44.0		44.0
${}^7\text{F}_0 \rightarrow {}^5\text{G}_2$	377–385	30.85	10.8	32.2	46.0	14.6	48.0
${}^7\text{F}_0 \rightarrow {}^5\text{G}_4, {}^5\text{G}_5, {}^5\text{G}_6$	370–377	33.5	50.2	35.0	40.1	54.3	40.6
${}^7\text{F}_1 \rightarrow {}^5\text{D}_4$	362–370	3.1		3.3	3.7		3.6
${}^7\text{F}_0 \rightarrow {}^5\text{D}_4$	355–363	16.9	22.1	18.9	20.0	22.2	19.4
${}^7\text{F}_0 \rightarrow {}^5\text{H}_3, {}^5\text{H}_4, {}^5\text{H}_5, {}^5\text{H}_6, {}^5\text{H}_7$	310–330	105.0	115.1	114.6	137.3	109.8	141.2

<sup>a</sup>Corrected from the Boltzmann equation.

lower symmetry of europium ions in crystal **II**. This effect is manifested in the  ${}^7F_0 \rightarrow {}^5D_2$  transition intensities shown in Table 3. A similar relation was also observed in the relative intensities of the  ${}^5D_0 \rightarrow {}^7F_2 / {}^5D_0 \rightarrow {}^7F_1$  transitions ( $R$ ) in the emission. The estimated  $R$  values for compounds **I** and **II** are 1.79 and 2.14, respectively.

The absorption spectra for both single crystals at 4 K are presented in Figs. 3 and 4. Fig. 5 compares the low (77 K) emission spectra for these two compounds. Lowering the temperature leads to the resolution of lines and shifts all the components by about  $10 \text{ cm}^{-1}$ . Moreover, one can isolate the components expected for the lower symmetry of the europium centres in crystal **II** in emission at 77 K. The fitting procedure for coordination polyhedra showed comparable and relatively high symmetries of the  $\text{Eu}^{3+}$  centres in both crystals ( $D_{4h}$  and  $D_{2d}$ ), however their different distortion and different splitting of levels (as a result of the strongest changes in M–O bond lengths) lead to different shapes of the spectral bands in both systems. The higher splitting of levels, at least for one metal center in tetragonal crystal **I**, is shown as a pronounced spread of bands in emission (see Fig. 5, bottom trace). Evaluation of the separated spectra for the respective europium centres needs selectively excited emission spectrum measurements and will be conducted in our future studies.

An analysis of Table 3 reveals a decrease in intensity with a temperature decrease to 4 K for compound **II**, especially in the region of the  ${}^7F_0 \rightarrow {}^5D_2$  and  ${}^7F_0 \rightarrow {}^5D_1$  transitions. Considering the depopulation of the  ${}^7F_1$  level

at low temperature one can expect an increase of intensity for the transitions from the  ${}^7F_0$  ground state to higher states. In contrast, we observed an almost unchanged intensity of  ${}^7F_0 \rightarrow {}^5D_0$  with decreasing temperature and a decrease in intensity for most other transitions. The above effect could be caused both by vibronic coupling and cooperative double excitation of coupled ions in the dimer. Separation of the intensities given by these mechanisms requires the investigation of diluted crystals.

Other striking observations concern the large differences in the splitting and separated component intensities versus temperature for crystal **I**. The 0–0 transition at 4 K is composed of three sharp lines, pointing to three different metal centres (see Fig. 3). This indicates a phase transition in the range 70–4 K. In the  ${}^7F_0 \rightarrow {}^5D_{1,2}$  transitions, at least nine and five components were found, which reveals an increase in the number of different symmetry centres, but still in tetragonal symmetry.

The excitation spectra of crystals **I** and **II** in the region of the  ${}^7F_0 \rightarrow {}^5D_2$  transition at 77 K show relatively strong vibronic components promoted by the internal ligand mode (namely  $\nu\text{-C=O}$ ) and by  $\text{MO}_8$  cluster motion. Some differences are seen in the spread and intensities of the components coupled with carboxylic group vibration. This is reasonable since, in both systems (dimeric and polymeric), a difference in carboxylic group coordination mode was shown on the basis of X-ray analysis. Moreover, these vibronic components are stronger in comparison with the respective components in the emission spectra, similarly as

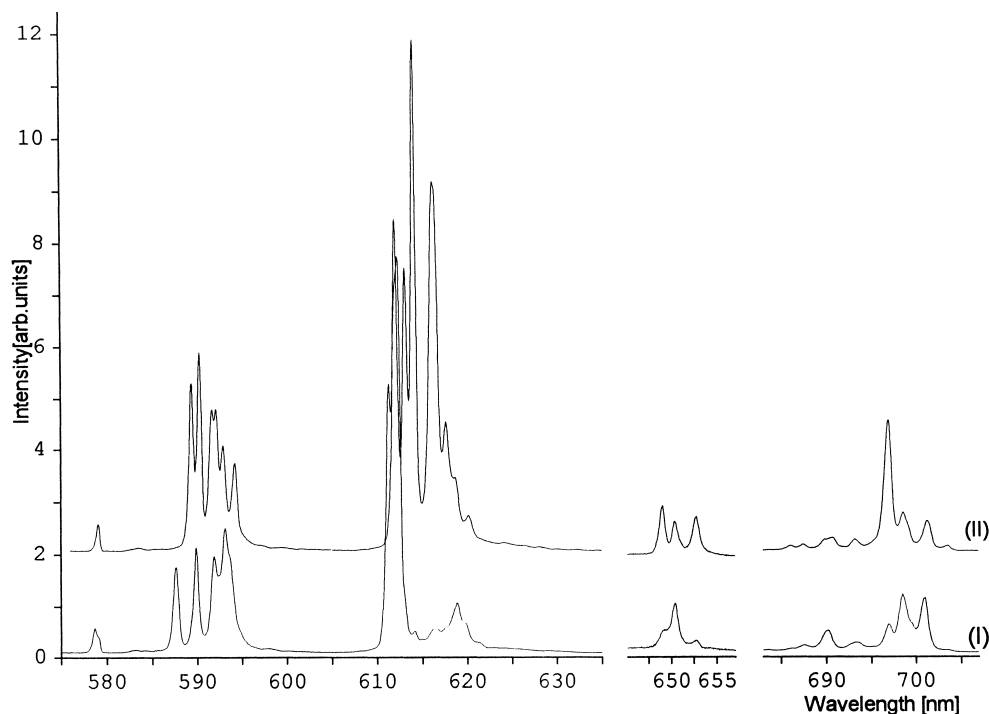


Fig. 5. Luminescence spectra of compounds **I** and **II** at 77 K.

described by other authors [14,15]. Besides, the splitting of bands given by the crystal field is drastically stronger in lower levels, i.e.  ${}^7F_J$  than  ${}^5D_J$ .

## References

- [1] J. Legendziewicz, *J. Appl. Spectrosc.* 62 (1995) 191.
- [2] E. Huskowska, J. Legendziewicz, *Polyhedron* 12 (1993) 2387.
- [3] J. Legendziewicz, E. Huskowska, *Excited States of Transition Elements*, World Scientific, Singapore, 1989, p. 228.
- [4] J. Legendziewicz, T. Głowiak, E. Huskowska, C.N. Dao, *Polyhedron* 7 (1988) 2495.
- [5] J. Legendziewicz, T. Głowiak, E. Huskowska, C.N. Dao, *Polyhedron* 8 (1989) 2139.
- [6] T. Głowiak, C.N. Dao, J. Legendziewicz, E. Huskowska, *Acta Crystallogr. C* 47 (1991) 78.
- [7] T. Głowiak, E. Huskowska, J. Legendziewicz, *Polyhedron* 11 (1992) 2897.
- [8] T. Głowiak, E. Huskowska, J. Legendziewicz, *Polyhedron* 10 (1991) 175.
- [9] G.M. Sheldrick, *Acta Crystallogr. A* 46 (1990) 467.
- [10] G.M. Sheldrick, SHELXL93. Program for the Refinement of Crystal Structures, University of Gottingen, Germany, 1993.
- [11] C.K. Johnson, ORTEPII. Report ORNL-5138, Oak Ridge National Laboratory, Tennessee, USA, 1976.
- [12] S.P. Sinha, *Structure and Bonding* 25 (1976) 69.
- [13] T. Głowiak, J. Legendziewicz, E. Huskowska, P. Gawryszewska, *Polyhedron* 15 (1996) 939.
- [14] M.T. Berry, A.F. Kirby, F.S. Richardson, *Mol. Phys.* 66 (1989) 723.
- [15] G. Blasse, *Int. Rev. Phys. Chem.* 11 (1992) 71.